Applied Energy 158 (2015) 86–96

Contents lists available at ScienceDirect

Applied Energy

journal homepage: www.elsevier.com/locate/apenergy

$NiO/CaAl_2O_4$ as active oxygen carrier for low temperature chemical looping applications

J.A. Medrano [a], H.P. Hamers [a], G. Williams [b], M. van Sint Annaland [a], F. Gallucci [a,*]

[a] Chemical Process Intensification, Chemical Engineering and Chemistry, Eindhoven University of Technology, De Rondom 70, 5612 AP Eindhoven, The Netherlands
[b] Johnson Matthey Public Limited Company, UK

HIGHLIGHTS

- A commercial Ni-based catalyst tested for low temperature chemical looping systems.
- The activation of the oxygen carrier has been studied in detail and explained.
- The redox activity has been measured for different fuel types and gas compositions.
- The catalytic activity for steam methane reforming has been evaluated.
- Kinetics for redox and catalytic processes has been well described.

ARTICLE INFO

Article history:
Received 14 April 2015
Accepted 17 August 2015

Keywords:
Hydrogen production
CO_2 capture
Membrane reactor
Chemical Looping
Ni oxygen carrier

ABSTRACT

The implementation of CO_2 capture systems in conventional processes has been proposed by the IPCC as an effective way to reduce anthropogenic CO_2 emissions. However, these capture systems may represent an important decrease in the global efficiency for conventional processes. Chemical Looping has already been demonstrated as a promising technology for more efficient CO_2 capture. Novel reactor concepts have been proposed in the literature, in which the reactions take place at lower temperatures with increased overall energy efficiency. However, few investigations have been carried out regarding the behaviour of oxygen carriers at relatively low operating temperatures. In this work, an active Ni-based oxygen carrier supported on $CaAl_2O_4$ inert material has been tested and characterized. The oxygen carrier has shown a promising behaviour for low temperature applications. However, it has been demonstrated that the oxygen carrier has to be pre-treated because of an interesting activation process which takes place only at high reduction temperatures. Oxygen carrier activation is caused by a reorganization of superficial nickel. Fresh oxygen carrier is covered by a layer of nickel with a strong interaction with the support. However, once the sample is reduced at high temperatures Ni is reorganized into small grains with reduced interaction with the support. This results in an enhancement in the reactivity and a higher oxygen transport capacity. After about 200 redox cycles, a small decrease in the solid conversion is observed due to agglomeration of the NiO grains. Nevertheless, the redox kinetics is still sufficiently fast for low temperature applications, provided that the oxygen carrier is pre-activated. The kinetics rates for the gas–solid reactions and gas-phase catalytic reactions have been determined, which can be used to predict the performance of the activated $NiO/CaAl_2O_4$ oxygen carrier for low temperature chemical looping applications.

1. Introduction

The increase in greenhouse gas emissions and its relation with climate change has brought general awareness that a reduction in anthropogenic greenhouse gas emissions is required for a sustainable future. Amongst all greenhouse gases affecting the Earth's climate, CO_2 has the largest contribution [1]. The CO_2 concentration in the atmosphere has increased dramatically over the last decades as a result of fossil fuels combustion for energy production.

In this context, different strategies have been proposed in order to reduce carbon dioxide emissions to the atmosphere. Most of them are related to a reduction in energy consumption,

* Corresponding author.
E-mail address: F.Gallucci@tue.nl (F. Gallucci).

http://dx.doi.org/10.1016/j.apenergy.2015.08.078
0306-2619/

substitution of fuel sources for renewable energy sources or CO_2 sequestration. An additional strategy that has been proposed for such reduction is Carbon Capture and Storage (CCS), which could account for up to 19% of the total reduction in emissions needed according to the IPPC and IEA reports when limiting the increase in the global average surface temperature to 2 °C [2,3].

The main objective of CCS is the production of a concentrated CO_2 stream that can be captured and subsequently kept in a suitable storage location for long time. The most energy intensive step in CCS is the capture of the CO_2. For CO_2 capture from fossil fuel power plants, the biggest concentrated emission sources, three main capture possibilities can be differentiated: post-combustion, oxy-fuel combustion and pre-combustion systems [4]. Amongst all possible strategies related to CCS, Chemical Looping (a sort of oxy-fuel combustion) is considered as the most efficient option with the lowest efficiency penalty [5,6].

The chemical looping technology is based on the redox activity of a (supported) solid with a high oxygen capacity, referred to as oxygen carrier, which is oxidized when in contact with air and subsequently reduced while supplying the oxygen needed for the conversion of a fuel. Because the combustion does not take place with direct contact with air, as in the conventional combustion, mixing of CO_2 with N_2 is intrinsically avoided and a concentrated CO_2 stream is obtained during the reduction of the oxygen carrier with the fuel. Thus, using the redox activity of the oxygen carrier the energy-intensive physical gas separation has been modified into an energy-wise less intensive mechanical gas–solid separation, which represents the main advantage of the chemical looping technology compared to other methods proposed for CO_2 capture. However, there is still an important lack of maturity of this technology, which represents its main drawback [7]. Up till now, research has been focused on experimental validation, modelling of the process and oxygen carrier evaluation, as described, e.g. in the review by Adanez et al. [8].

Chemical Looping has not only been proposed for power production but also for fuel gas reforming. For this application, the concept is named Chemical Looping Reforming and the product is not electricity but syngas [9,10]. In a possible reactor configuration for both Chemical Looping systems, the oxygen carrier is circulated between two interconnected fluidized bed reactors. First, the reduced solid (Me) is oxidized in the air reactor with air by a highly exothermic reaction. This hot oxidized material (MeO) is then transferred to the fuel reactor, where it is put into contact with the fuel. Reaction between oxygen and fuel leads to a reduction of the metal oxide and the solid needs to be regenerated. Thus, the reduced material is again transferred to the air reactor, where it is oxidized to start another cycle. By adjusting the solids circulation rate, and hence the amount of oxygen in the fuel reactor, the system can be operated for either fuel combustion (CLC) or fuel reforming (CLR).

The potential of this technology has not only been limited to CLC or CLR systems. In fact, Chemical Looping has been adapted for other applications such as hydrogen production in the Chemical Looping Hydrogen (CLH) concept [11,12] and fuel gasification in Chemical Looping Gasification [13]. Recently, two new derived concepts have been proposed in the literature for more efficient use of Chemical Looping systems: Packed Bed Chemical Looping Combustion (PB-CLC) concept for operation at elevated pressures [14] and the Membrane Assisted Chemical Looping Reforming concept for ultra-pure hydrogen production with integrated CO_2 capture [15].

In the PB-CLC concept (Fig. 1 left), methane or syngas obtained from conventional gasification of coal or biomass is used as fuel. Exploiting the dynamically operated packed beds, the separation of gas and solids via cyclones is avoided and the process can be relatively easily operated at elevated pressures, which is required to obtain high process efficiencies [14,16]. A continuous process can be obtained by operating several packed bed reactors in parallel. Three different main operating steps are distinguished: (I) reduction, (II) oxidation and heat generation and (III) heat removal. Different operating strategies have been proposed for optimal heat management depending on the oxygen carrier reactivity [14,17]. In one of the strategies, an oxidized oxygen carrier is reduced at about 450 °C (I) and afterwards, the reactor is purged with N_2 and oxidized with air (II). During oxidation, the reactor temperature rises to 1200 °C. When the bed is completely oxidized, air is heated in the reactor from 450 °C (the adiabatic temperature rise when pressurizing air from ambient conditions to 20 bar) to 1200 °C (III), which is fed to the gas turbine for power production. When the heat has been removed from the reactor, the packed bed is again at 450 °C and after a purge with N_2, the oxygen carrier can be reduced again. For this operating strategy, an oxygen carrier is required that is reactive with H_2 and CO at low temperatures (450–600 °C), but can withstand the high temperatures (1200 °C)

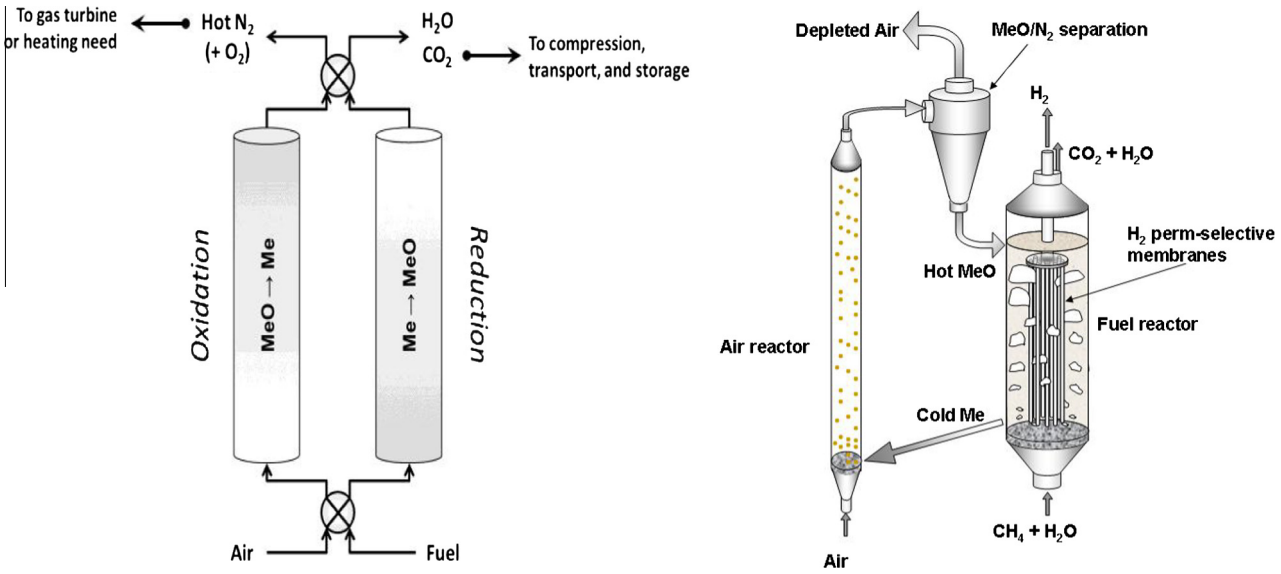

Fig. 1. Left: schematic representation of the PB-CLC concept [18]. Right: Schematic representation of the MA-CLR concept.

during the oxidation step. So far, nickel-based oxygen carriers have been identified as one of the most promising oxygen carriers, because of the low melting point of copper and the high active weight content required for manganese and iron based oxygen carriers [14].

In the MA-CLR concept (Fig. 1 right), Pd-based selective membranes for H_2 separation are immersed in the fuel reactor. When methane is used as fuel for the steam methane reforming process (SMR), the produced hydrogen is directly extracted from the bed resulting in a shift of the equilibrium towards the products (Le Châtelier's principle), allowing also the integration of the water gas shift reaction (WGS). At the outlet, stream of the fuel reactor will mainly contain CO_2 and H_2O, which can be easily separated by steam condensation, while an ultra-pure H_2 stream is produced through the membranes. This novel concept achieves a high degree of process intensification compared to the traditional steam methane reforming process for H_2 production. The optimal temperature in the fuel reactor for this application is around 600 °C [15] with a steam to carbon ratio (S/C) of two. At this temperature the performance of the selective Pd membranes is maximized and thermodynamic equilibria can be completely shifted. Moreover, at this temperature a compromise between the highly endothermic SMR reaction and the exothermic WGS reaction is obtained, where full CH_4 conversion can be achieved resulting in an efficient use of the fuel. In this concept, the behaviour of the solid becomes critical for a good performance in the fuel reactor. This is mainly related to the fact that in this reactor gas–solid reactions and catalytic reactions take place at the same time. When the solid behaves as an oxygen carrier (gas–solid reaction), the small amount of oxygen transferred from the air reactor is used for partial oxidation of methane in order to sustain the temperature needed in the reactor. Furthermore, when the solid is fully reduced it behaves as a catalyst for the SMR process (catalytic reaction). Thus it is important to find a solid able to combine both properties, making it suitable for the concept.

Both proposed reactor concepts have in common that a good activity of the oxygen carrier for reduction and reforming at low temperatures are needed or desired. However, up till now all Chemical Looping applications have been carried out at relatively high temperatures. Due to this fact, there is still an important lack of knowledge about the behaviour of oxygen carriers in low temperature applications (400–700 °C). Thus, in this work it is aimed the proposal of an active oxygen carrier that can be used for novel concepts, all carried out at low temperatures. Ni, Cu, Fe and Mn based metal oxides are the most studied oxygen carriers in Chemical Looping systems, where more than 700 oxygen carriers have already been developed and tested [8]. At low temperatures, Ni-based materials show high oxygen carrier conversions and high selectivities to the desired products. For Cu-based oxygen carriers the product selectivity is also very high. The advantage of nickel for the MA-CLR concept is that it is also a well-known catalyst for the steam methane reforming [19]. Both metals have high oxygen capacity and the total amount of active content needed is not high. Fe-based oxygen carriers show low selectivities in case of high degrees of reduction and also poor CH_4 conversions. Mn-based oxygen carriers have also low oxygen contents and are therefore not considered interesting for low temperature applications. Concluding, when comparing the different oxygen carriers for low temperature chemical looping applications, Ni-based oxygen carriers might be the most interesting and therefore this material has been selected in this work.

For the selection of the support, it is important to consider different characteristics that might influence its performance, in particular agglomeration and interactions between the active metal and the support [20]. In most of the used Ni-based oxygen carriers, Al_2O_3 was selected as support. However, the formation of nickel aluminates has been mentioned in the literature as one of the main problems. When $NiAl_2O_4$ is formed, the reactivity is strongly reduced compared to free NiO. Consequently, the use of aluminates as support has been proposed as a suitable solution for the prevention of the formation of nickel aluminates during the oxidation step. In this study, $CaAl_2O_4$ has been selected as support, which has only been used for high temperature Chemical Looping applications, where a very high reactivity, good regenerative properties and a high selectivity for methane combustion to CO_2 and H_2O were achieved [21]. However, all this properties abovementioned are not conclusive for much lower temperatures and thus it is important to have a better understanding of its performance under these more stringent conditions (in terms of reactivity). The combination of Ni supported on $CaAl_2O_4$ is a well know catalyst for steam reforming processes and it is commercially available. Due to this reason, in this work a commercial catalyst has been used instead of a newly developed oxygen carrier, thus gaining a rapid availability of the solid when needed and more homogeneous properties.

Thus, the main objective and motivation of this work is to study the suitability of a commercial catalyst (described in Section 2) used for Steam Methane Reforming as a potential oxygen carrier for low temperature applications. The novelty of this study is in line with the development of novel Chemical Looping concepts operated at low temperatures. Due to the lack of study on oxygen carriers working at low temperatures, in this work the reactivity of an oxygen carrier at temperatures is studied at temperatures ranging from 500 °C to 700 °C. Furthermore, during this work it has been discovered that this oxygen carrier behaves differently when it is used at low temperatures and when it is used at higher temperatures. This comes along with an activation occurring in the surface of the solid. This activation, which is investigated in Section 3 and which procedure is described, gives to this work extra-novelty combined with reactivity tests at low temperatures. The document is divided into three different parts. First, a deep oxygen carrier characterization is carried out throughout different characterization techniques for the explanation of the activation observed. Secondly, gas–solid kinetics are determined in TGA at different oxidation/reduction conditions. Finally, as the completely reduced oxygen carrier behaves like a catalyst for steam methane reforming reaction, catalytic kinetics is determined for the reduced oxygen carrier in a differential packed bed reactor by comparison with data from the literature. In this case the catalytic kinetics is not fitted into a new expression but experimental results are compared with another kinetics proposed in the literature under similar experimental conditions. In the end the work is summarized with main conclusions regarding the use of a commercial catalyst as oxygen carrier for novel low temperature Chemical Looping applications.

2. Materials and methods

2.1. Oxygen carrier and characterization

A Johnson Matthey product, HiFUEL® R110 (Ni-based catalyst supported on $CaAl_2O_4$ for steam reforming of natural gas), available in pelleted form from Alfa Aesar, is tested and evaluated as a suitable oxygen carrier for Chemical Looping applications at low temperatures. For the experimental tests, the pellets are crushed to the desired particle size and the content of (available) Ni is determined by complete reduction and oxidation of the samples. The oxygen carrier conversion (X_s) is subsequently calculated through the mass change in the oxygen carrier under different experimental conditions, defined by Eq. (1), where m is the current mass and m_{ox} and m_{red} are the mass of the fully oxidized and reduced forms of the oxygen carrier.

$$X_s = \frac{m - m_{red}}{m_{ox} - m_{red}} \quad (1)$$

The main properties of the oxygen carrier have been analyzed through different characterization techniques for fresh material and after-used samples. The particle density is measured in a Quantachrome Ultrapyc 1200e. The surface area of fresh and used material was determined by the Brunauer–Emmet–Teller (BET) method by adsorption/desorption of nitrogen at 77 K in a Thermo-Scientific Surfer. In addition, the microstructure of the different samples was analyzed in a Phenom scanning electron microscope (SEM).

Crystalline species were identified by X-ray Diffraction (XRD) in a Rigaku (WAXS) diffractometer at 298 K with a mobile Cu anode. The diffractometer uses a graphite monochromator to select Cu Kα radiation and all experimental measurements have been carried out by varying the diffraction angle between 10° and 90°.

X-ray photoelectron spectroscopy (XPS) data were recorded on a Kratos AXIS Ultra spectrometer equipped with a monochromatic Al Kα X-ray source and a delay-line detector (DLD). Spectra were obtained using an aluminium anode ($h\upsilon$ = 1486.6 eV) operating at 150 W, with survey scans at constant pass energy of 160 eV and region scans at a constant pass energy of 40 eV. The background pressure was $2 \cdot 10^{-9}$ mbar. CasaXPS data processing software was used for peak fitting and quantification, where all binding energies were referenced to the C 1s line at 284.6 eV. Surface composition were estimated from the integrated intensities corrected by the atomic sensitivity factors [22].

Finally, temperature programmed reduction (TPR) analyses were carried out for different samples in a Rubotherm Dyn THERM MP HT-II instrument equipped with a magnetic suspension balance. The sample was heated at 7 °C/min from room temperature to 1000 °C with a flow rate of 20 mL/min and 10% H_2. The consumption of hydrogen was then calculated in order to identify possible components in the samples.

2.2. Gas–solid kinetics in TGA

Thermogravimetric analyses (TGA) have been carried out in order to evaluate the gas–solid kinetics of the oxygen carrier (the schematic representation of the experimental setup is reported in Fig. 2). The TGA consists of a cylindrical quartz glass reactor (15 mm i.d.) placed in an oven that can operate at up to 1000 °C and atmospheric pressure. The sample (typically 100 mg) was placed in a quartz sample-holder (40 μm pore size) connected to a Sartorius balance with a platinum wire. Temperature and weight of the sample, which is the key parameter for gas–solid kinetics determination, are continuously monitored. Gas flow rates are controlled by Mass Flow Controllers (Bronkhorst) and the gas is fed from the bottom part of the reactor. A permanent nitrogen purge stream is fed to the balance to avoid exposure of the balance electronics to reactive species, but this stream is not in contact with the sample. Lines at the outlet of the TGA are traced in order to avoid steam condensation.

Reactivity experiments are carried out using H_2, CO (mixed with CO_2) and CH_4 (mixed with steam) as reducing agents (N_2 balance)

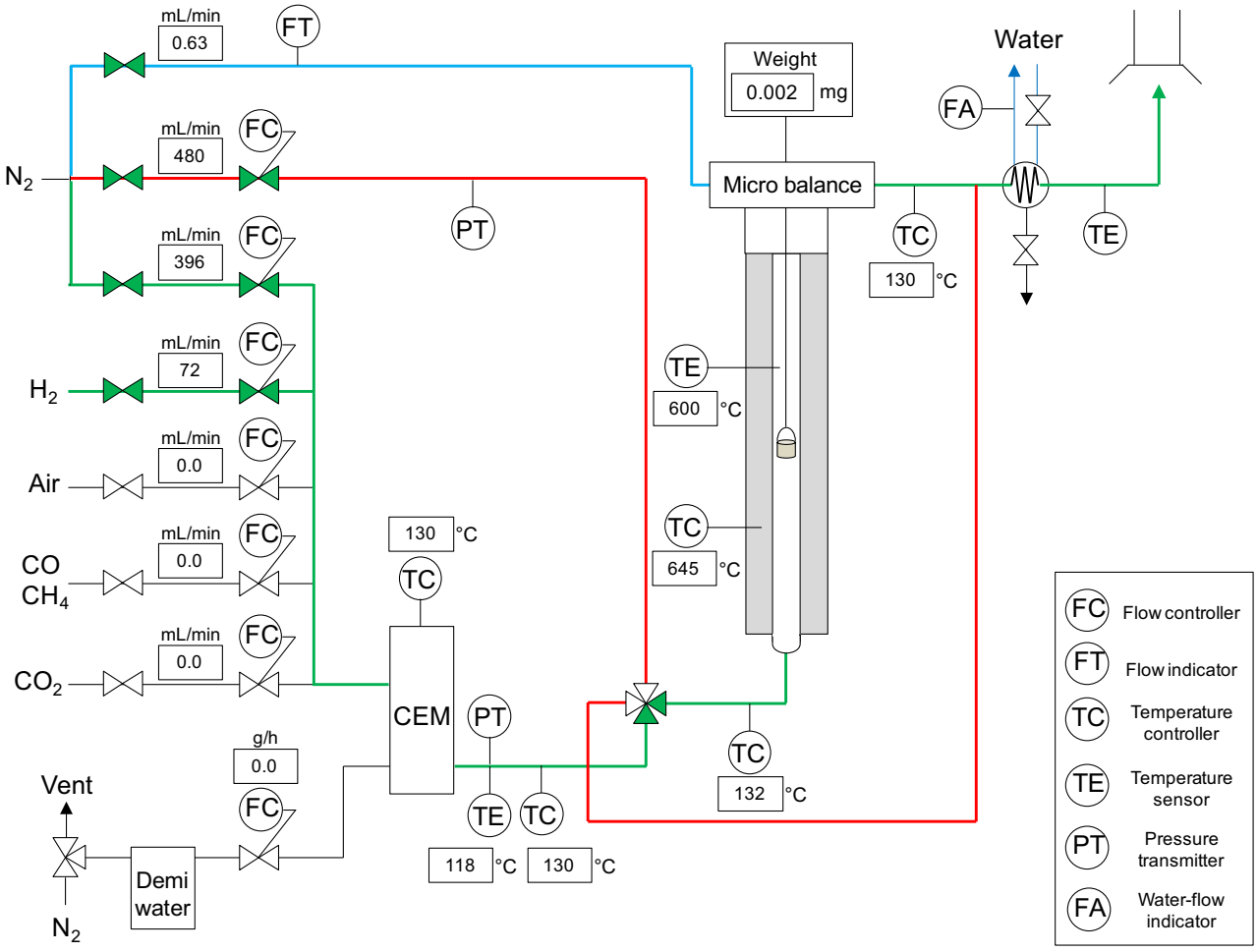

Fig. 2. TGA setup used in this work.

and air during oxygen carrier oxidation. Temperatures between 500 °C and 800 °C have been used under different total flow rates and gas compositions. Prior to an experiment, the temperature is increased to the desired value at a constant heating rate and inert flow conditions (nitrogen) and, after that, consecutive cycles of reduction and oxidation are carried out at the desired conditions. Two minutes purge (in nitrogen atmosphere) between reduction and oxidation is always applied in order to avoid mixing of the different reactants. A minimum of five reduction–oxidation cycles at the desired conditions have been evaluated to verify cyclic reproducibility of the results. Tests with different total flow rates and with samples with different particle sizes have demonstrated that no external mass transfer limitations were observed and also no internal mass transfer limitations for particle sizes up to 300 μm. As reference case, experiments are carried out under a total flow rate of 480 mL/min using samples with 200–300 μm particle size. A summary of the conditions used for the gas–solid kinetics determination is given in Table 1.

2.3. Catalytic kinetics in a batch fixed-bed reactor

As discussed during the introduction, when the oxygen carrier is fully reduced it will behave as a catalyst in the fuel reactor of the MA-CLR concept. Thus it is not only important to study gas–solid kinetics in the TGA, but also the catalytic activity (kinetics) for Ni/$CaAl_2O_4$. For this study a small packed-bed reactor has been used for kinetic measurements for the catalytic gas phase reactions (steam methane reforming and water gas shift reactions). The catalyst bed consists of 1 g of fully reduced oxygen carrier (200–300 μm particle size) mixed with 1 g of inert material (quartz) with the same particle size and is placed in a U-shaped quartz reactor (8 mm i.d.) where the temperature is controlled by an electrical oven (Fig. 3). Inlet gas flow rates are controlled by Brooks Instruments mass flow controllers, whereas steam is controlled by a C.E.M. The outlet gas composition is continuously analyzed in an IR and heat conductivity analyzer (Sick) once all steam has been condensed in order to avoid water condensation in the analyzer.

The catalytic activity of the oxygen carrier for the steam methane reforming process is evaluated at temperatures between 500 and 700 °C. Different steam-to-carbon (S/C) ratios, CH_4 concentrations and total flow rates have been used. Before the experiments are started, the samples are heated at a constant heating rate of 5 °C/min under nitrogen atmosphere. Then the sample is reduced with 20%v/v H_2 and a total flow rate of 600 mL/min during 1 h (N_2 balance). After this reduction, the maximum degree of reduction is reached. Therefore, all the reactions that take place during the tests are only related to the catalytic reaction with nickel and not to gas–solid redox reactions. After the reduction, and 5 min purge in N_2 atmosphere, CH_4 is fed together with steam at the desired composition (N_2 balance) for the SMR reaction. In the case of WGS reaction, CO_2 is fed together with H_2 at different compositions (N_2 balance). The operation is carried out until steady state operation is reached. After that, the amount of carbon deposition is evaluated with diluted air (10% O_2) by determining the total formation of CO_2 and CO.

3. Results

3.1. Reactivity tests

For both reactor concepts abovementioned, the oxygen carrier needs to present fast kinetics at relatively low temperatures. For instance, the PB-CLC concept works during the reduction step at 450–600 °C and at these temperatures no reported reactivity data are available. On the other hand, the MA-CLR concept has an optimum temperature of around 600 °C in order to maximize the hydrogen recovery. In this concept the oxygen carrier combines gas–solid reactions and gas-phase catalytic reactions, thus the

Table 1
Experimental conditions used in this work for redox kinetics determination in the TGA.

	Temperature (°C)	Total flow rate (mL/min)	Inlet gas composition	Conditions respective cycle
Reduction with H_2	500–800	480	5–50% H_2 (N_2 to balance)	Oxidation at 700 °C with air
Reduction with CO	500–800	480	5–40% CO CO_2/CO = 2 (N_2 to balance)	Oxidation at 700 °C with air
Oxidation with O_2	500–800	480	2–21% O_2 (N_2 to balance)	Reduction at 700 °C with 20% H_2

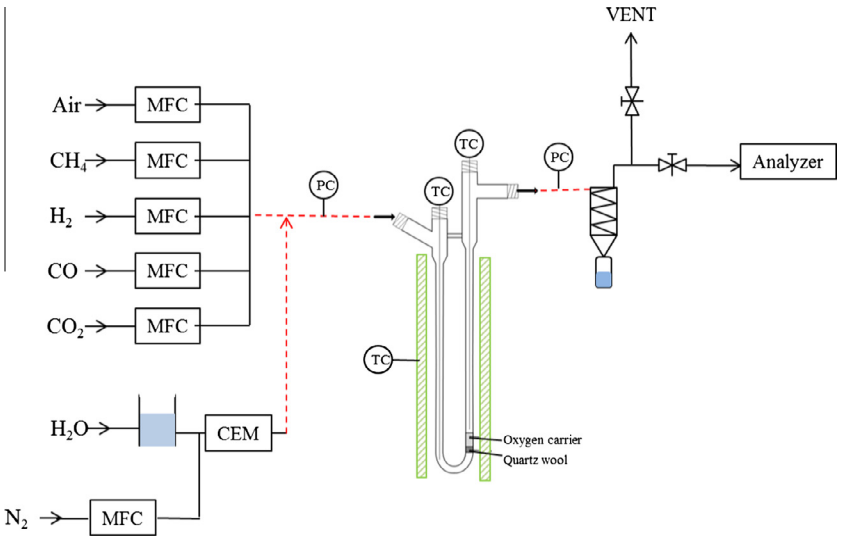

Fig. 3. Kinetic setup used in this work.

solid should show high activity for both systems at the low temperatures aimed for the concepts.

During reactivity experiments, fresh material was tested in the TGA with H_2 as reducing agent at different temperatures. The maximum tested temperature was 900 °C and, at such conditions, the maximum degree of reduction was measured. This value indicated a NiO content of 20 wt%. The results were reproducible, but the reduction reactivity was found to depend on the operating conditions of the previous cycles. The oxygen carrier conversion during the reduction with 20% H_2 at 700 °C is depicted in Fig. 4 for the same sample with a different temperature history. The so-called fresh material has been tested only at relatively low temperatures of 700 °C, while the activated one is the same sample once it has been tested under reacting conditions at high temperatures above 900 °C before carrying out the experiment at 700 °C. As can be observed, the oxygen carrier reactivity is strongly increased as a result of the high temperature tests. The maximum conversion is also clearly increased and, moreover, faster kinetics was observed.

The oxygen carrier has been thoroughly characterized (Section 3.2) to investigate and explain this behaviour. When fresh material is directly oxidized at high temperatures (no oxygen carrier reduction), the behaviour of the oxygen carrier is similar to a fresh sample. This implies that the activation of the oxygen carrier is caused by its reduction at high temperatures. Finally, the reversibility in the change of the behaviour was verified. Therefore, the oxygen carrier was tested over more than 200 redox cycles and only a small decrease of 8% in the final maximum conversion was observed, while the initial slope (thus the initial kinetics) remained unchanged.

Methane was also used as reducing agent in TGA reactivity tests, since methane is the fuel used in the MA-CLR concept. CH_4 was fed together with sufficient H_2O in order to avoid carbon formation (S/C-ratio of 3) and the results are shown in Fig. 5. The oxygen carrier did not show activity at low temperatures when the sample was fully oxidized. Only when the sample was not fully oxidized (i.e. it contained some remaining reduced oxygen carrier), reduction with CH_4 was observed. In these experiments the sample was previously oxidized at 700 °C with 5% O_2 and a total flow rate of 480 mL/min during different times in order to determine the exact amount of reduced oxygen carrier in the sample. As it can be observed, only when there is some free metallic Ni in the sample, the reduction of the oxygen carrier with methane takes place. This is explained by the fact that Ni is a catalyst for the steam methane reforming process and hence, prior to the reduction of the oxygen carrier, the gas-phase catalytic reaction occurs. In this catalytic reaction CO and H_2 are produced and they are the responsible for the reduction of the oxygen carrier. Fully oxidized oxygen carrier does not react with methane at 700 °C. However, when 11% of the nickel is in the form of free Ni, catalytic reactions can take place and the reduction of NiO starts with the formed H_2 and CO. However, there is a dependency on the total amount of free Ni needed to reduce the oxygen carrier as a function of the temperature. As can be discerned from Fig. 5, when the same amount of free Ni is present in the sample, but the reduction is carried out at 500 °C, there is hardly any reactivity. Only if the total amount of free Ni is increased, catalytic reactions can take place. For that reason, kinetics with CH_4 as reducing fuel has not been further studied for this oxygen carrier.

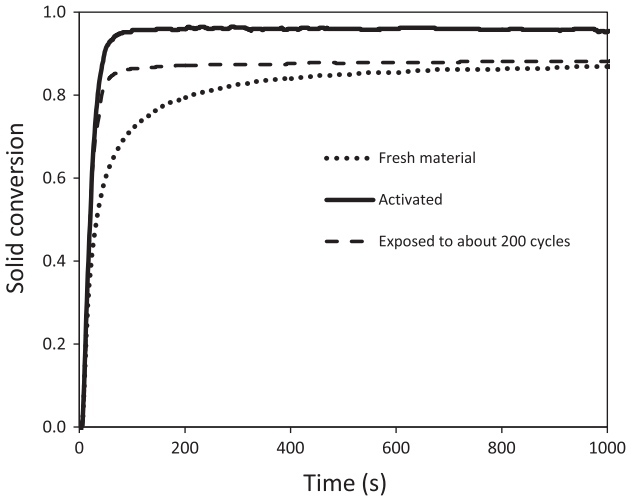

Fig. 4. Oxygen carrier conversion for reduction with 20% H_2 at 700 °C for different samples ($NiO/CaAl_2O_4$).

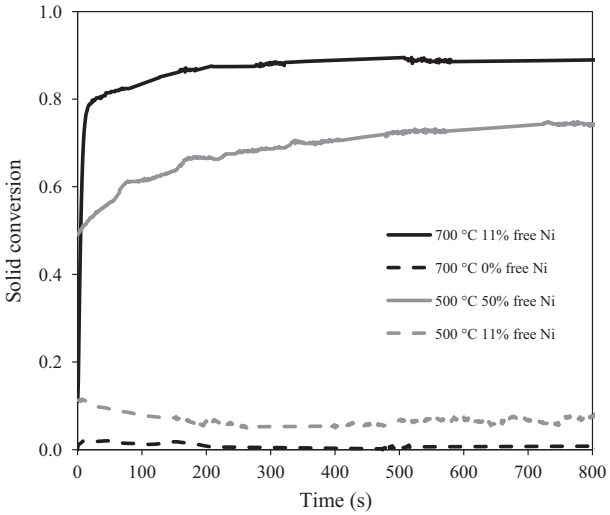

Fig. 5. Oxygen carrier conversion for reduction with 20% CH_4 and 60% H_2O at different temperatures for activated material ($NiO/CaAl_2O_4$).

Since it has been demonstrated that the activated material has a better performance, all subsequent reactivity experiments were carried out with activated material. However, prior the determination of the gas–solid kinetics in TGA and gas-phase kinetics in packed bed reactor, the activation observed for the solid is analyzed and explained through characterization of different samples of the solid.

3.2. Oxygen carrier characterization

The main activation of the oxygen carrier can be observed through TPR results (Fig. 6). For the fresh sample, it is possible to identify an intense reduction peak at around 800 °C which is directly correlated to the activation of the oxygen carrier. The TPR results of activated material show different profiles. These results are in agreement with results obtained by Cabello et al. [23] for a similar oxygen carrier. Thus, it is demonstrated that if the oxygen carrier is directly used at temperatures around 500–700 °C, which are desired for low temperature Chemical Looping concepts, its behaviour would be completely different compared to when it is first activated at high temperatures.

In order to explain why the oxygen carrier behaviour is modified when reduction is carried out at high temperatures, three different samples have been characterized in detail. The main results of the characterization have been summarized in Table 2. Fresh sample is referring to a sample taken from pellets crushed to the desired particle size, where the sample has never been exposed to reacting conditions after its preparation. Activated material is referring to samples that have been reduced during several cycles

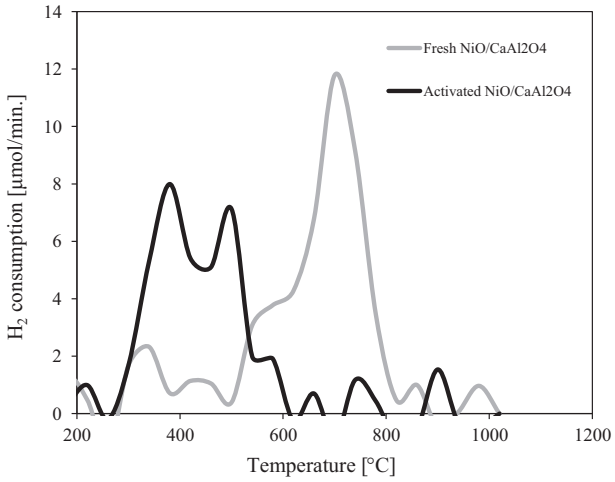

Fig. 6. TPR profiles of fresh and activated $NiO/CaAl_2O_4$ material.

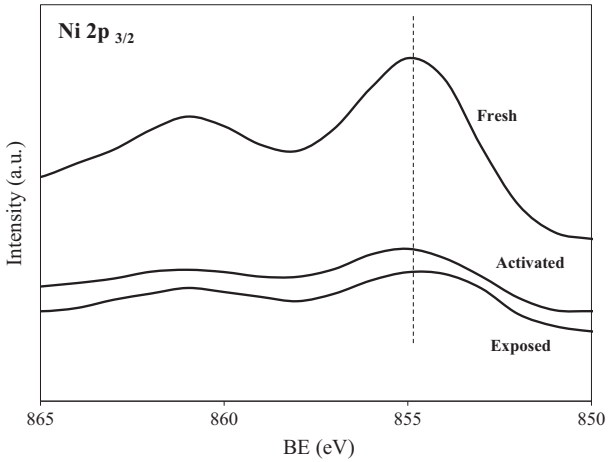

Fig. 7. XPS analysis for fresh, activated and exposed oxygen carrier ($NiO/CaAl_2O_4$) to more than 200 redox cycles.

Table 2
Main properties of the oxygen carrier.

	Fresh	Activated	Activated and exposed to more than 200 cycles
S_{BET} (m^2/s)	23.3	21.2	18.1
Mean pore size (nm)	15	11.8	12.4
Particle density (kg/m^3)	3451	3487	–
XRD (main compounds)	NiO, Al_2O_3, $CaAl_2O_4$, $CaAl_4O_7$		
XPS. Ni 2p (%)	10.6	3.2	2.5

at 900 °C and that show an improved performance compared to fresh material. The third sample has been activated and exposed to more than 200 redox cycles and has shown a slight decrease in the final oxygen carrier conversion.

First, the sample is characterized by means of pore size, particle density and crystalline species in order to evaluate the possible structural changes in the sample caused by the activation. According to the results reported in Table 2, there is not a significant change in the morphological structure of the particles since the superficial area remains almost constant and the mean pore size is not increasing.

Migration of Ni species from the bulk to the surface or vice versa could also explain the observed activation of the oxygen carrier. Therefore, XPS analyses have been carried out to determine the surface composition. The results show unexpected losses of superficial nickel in the oxygen carrier once it has been activated. Hence, Ni migration from the bulk to the surface cannot be responsible for the observed activation. In addition, also a decrease in the superficial content with respect to the activated material was observed once the sample had undergone numerous reduction–oxidation cycles. This can be related to agglomeration of the Ni. Another important aspect observed in the XPS analyses is the fact that the binding energy for Ni^{2p} is strongly reduced from the fresh to the activated material (Fig. 7). This might indicate the main cause of the activation, which is correlated with the Ni-support interactions. This strong Ni-support interaction is not caused by the presence of nickel aluminates, because they have not been detected in the XPS measurements for any sample. Moreover, this is in agreement with results obtained during XRD analyses. Hence, it can be concluded that the use of the spinel $CaAl_2O_4$ as support avoids the formation of less reactive nickel aluminates. The XPS analyses are in line with literature [23].

It has been concluded that the activation of the oxygen carrier is not caused by either structural changes or increase in Ni concentration on the surface. However, a significant decrease in the surface Ni concentration has been observed after the sample was activated. This indicates the possibility of a different interaction or reorganization of the Ni with the support. This has also been evaluated by taking SEM images of the different samples (Fig. 8). For all samples, nickel was in the form of NiO. For the fresh sample it is possible to observe the presence of a well distributed and homogeneous NiO layer (white) on the support. This layer has a strong interaction with the support (as observed during XPS analysis) and is assumed to be caused by the preparation method of the catalyst. However, for the activated sample, Ni is reorganized into small spots with a small grain size. It implies that there is a modification in the superficial organization of the nickel. This is also explained by the differences in the binding energy measured with XPS, which decreases once the sample has been activated. Thus, the activation is believed to be caused by the reorganization of the active component on the support. Mile et al. [24] already determined the presence of different NiO forms in silica-supported catalysts. The presence of a bi-dimensional NiO monolayer covering the top of the support with a strong interaction implies a less reducible NiO for TPR experiments. This explains the fact that fresh oxygen carrier is less active compared to the activated sample. However, once the oxygen carrier has been reduced at high temperatures there is a reorganization of the monolayer NiO into small NiO grains, which show higher activities for reduction (confirmed by BE in XPS). SEM images for the activated samples after more than 200 reduction–oxidation cycles show bigger NiO grains. This confirms Ni agglomeration over time, which reduces the active amount of reducible NiO (confirmed by XPS). Nevertheless, after even more cycles, solid conversion was not decreasing anymore and further agglomeration was not observed. However, this exposed sample has still NiO in the form of grains. Due to this fact, the reactivity is the same as for the just activated sample, as shown in Fig. 4. Moreover, the decrease observed in Ni concentration in XPS analysis after activation can be explained by this reorganization of the superficial NiO. XPS measures a fixed small spot window. Thus under the presence of a NiO layer in the fresh material, the coverage is higher than the small grains for activated sample. Therefore, this higher coverage will imply a higher content of NiO in the sample.

As a summary of the characterization carried out in this work, it has been determined that activation of the oxygen carrier should be done in order to provide full reduction of the Ni at low temperatures (TPR). This activation takes place only when the solid is exposed at temperatures around 900 °C under reducing conditions. Thus prior starting experiments, a procedure based on reduction of

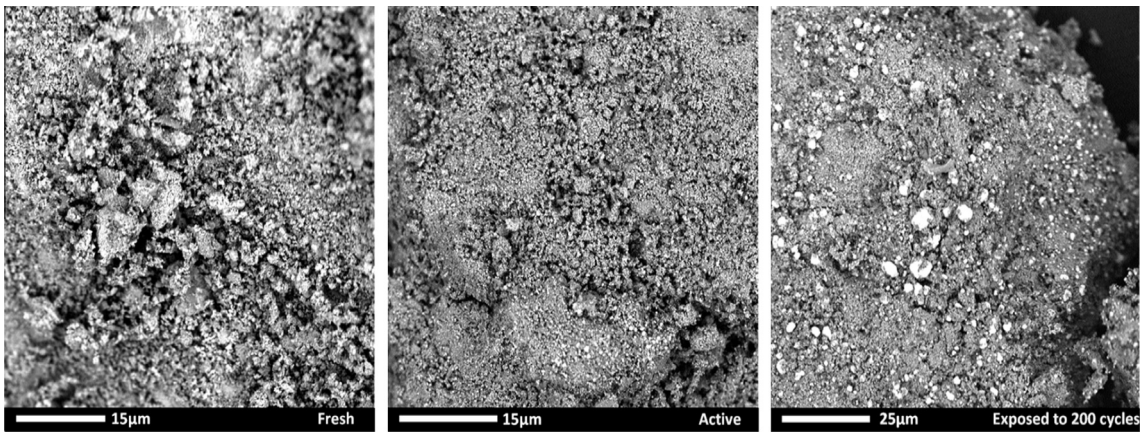

Fig. 8. SEM pictures for different samples of the oxygen carrier ($NiO/CaAl_2O_4$). Left: fresh material. Centre: activated material. Right: Material exposed to more than 200 redox cycles.

the solid at 900 °C should be done providing that there is full reduction conversion of the solid. Before this activation, the NiO layer is covering part of the superficial Ni that is available for reaction. Therefore, conversions achieved with fresh material are far from full oxygen carrier conversion. Nevertheless, once it has been activated, Ni in the surface is more accessible for gas–solid reactions and oxygen carrier conversion is clearly improved.

3.3. Fixed bed operation

The improvement in oxygen carrier conversion has been proven after solids activation. This has lead into a more accessible superficial Ni. Therefore, it might be thought that during the gas-phase reaction (catalytic activity when Ni is fully reduced), the maximum fuel conversion achieved at the outlet of the reactor will be increased. This is of interest for the MA-CLR concept and, in order to verify it, different experiments have been carried out in a small packed bed reactor. In this case, activated and fresh particles have been tested separately. An example of CH_4 conversion is shown in Table 3 for different S/C-ratios and different inlet compositions for the fresh and activated particles. In this case, a temperature of 600 °C has been used with N_2 to balance. It is clearly demonstrated that the activation of the oxygen carrier leads to an increase in the final CH_4 conversion achieved. According to the results depicted in the table, this activation is more important when the conditions are unfavoured for achieving high conversions, like observed in the cases of low Steam-to-Carbon ratio or for high inlet fuel concentrations. Actually, it is observed a clear trend in the improvement of the conversion as a function of the experimental conditions. The higher the Steam-to-Carbon ratio, the lower is the increase associated to the use of activated catalyst, and also the higher the inlet concentration of CH_4, the higher is the increase in the improvement. The fact that the conversion is increased demonstrates that there is a modification in the grain size of the superficial Ni and that it becomes especially important for the most unfavoured cases. This has been confirmed with the SEM analyses and implies that Ni is more accessible for the reaction. Moreover, these results are in agreement with gas–solid reactivity studies in the TGA, since for that case, the oxygen carrier conversion is also increased when using the activated particles. However, during the present experiment only gas-phase catalytic reaction takes place.

Table 3
CH_4 conversion in a small packed bed reactor for steam methane reforming reaction when using activated and non-activated material.

Conditions			CH_4 conversion		
T (°C)	S/C	$C_3H_{8,0}$ (%v/v)	Activated	Non-activated	Improvement (%)
600	2	12	49.0	43.2	13.6
	3	12	54.8	50.6	8.4
	4	12	61.1	59.3	2.9
	3	8	60.8	57.1	6.4
	3	16	50.4	44.0	14.5

3.4. Kinetics for gas–solid and catalytic reactions

A different reactivity was observed with this material compared to previous reported redox reactions with NiO/Ni oxygen carriers in the literature [25,26], especially because this oxygen carrier has never been used at such low temperatures. Therefore the kinetics of the activated oxygen carrier has been determined for the reduction reactions with CO and H_2 and the oxidation with O_2. The kinetics has been determined in the TGA with particles that were crushed to 200–300 μm particle size with the procedure that has been explained in Section 2.2. No internal mass transfer limitations were measured with the selected particle size and absence of external mass transfer limitations were assured by the relatively high flow rates, therefore true kinetics was measured. TGA experiments have shown that the reduction kinetics depend on the temperature at which the previous oxidation cycle was carried out. This effect has been excluded by performing the previous oxidation always at 800 °C as it is expected that this temperature is reached in the air reactor in the MA-CLR process. The oxidation kinetics has been evaluated by experiments carried out after a reduction at 700 °C with 20% H_2 in the inlet composition. With these conditions, the experiments were reproducible, which has been verified by performing every experiment for at least three times.

During the reductions, the reactant fraction and temperature have been varied between 5–50% and 500–800 °C, respectively. For the reductions with CO, some CO_2 (CO_2/CO-ratio of 2) has been added to avoid carbon deposition. For the oxidation, the maximum O_2 fraction is 21% (O_2 fraction in air) and a temperature of 600–800 °C has been varied. The desired gas fractions have been obtained by dilution with N_2. All the experiments have been performed at atmospheric pressure.

From the solid conversion curves from the TGA experiments an active weight content of 20 wt% NiO has been derived. The markers in Fig. 9 show the solid conversion as a function of time on stream for the different operating conditions. It appears that during reduction the reaction rates decrease with the solid conversion. At lower temperatures, it is even not possible to get full conversion of the

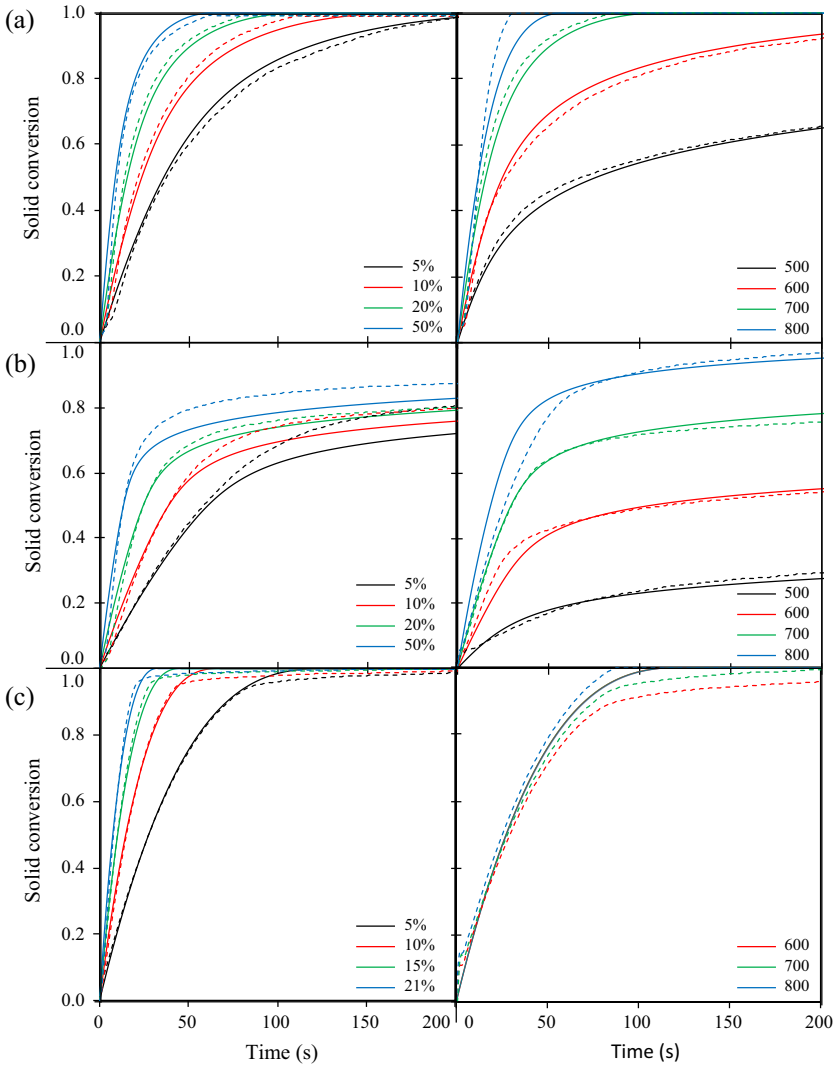

Fig. 9. An overview of the experimental data from the TGA (dashed lines) compared with the derived kinetics (lines). Left part: influence of gas composition; right part: influence of temperature. (a) Reduction with H_2 (left: T = 700 °C; right: 20% H_2), (b) reduction with CO (left: T = 700 °C; right: 15% CO_2), (c) oxidation with air (left: T = 800 °C; right: 21% O_2). All the experiments have been carried out at atmospheric pressure.

NiO. This behaviour has been described by a shrinking core model with a mixed control of chemical reaction and diffusion, which is summarized in Table 4. Experiments with larger particles did not show a different slope in the second part of the curve, which means that it is questionable if the observed decrease in the reaction rate is indeed caused by diffusion limitations. Thus, although this model is often used in literature and gives a good description of the observed kinetics, the underlying assumptions may not be fully correct.

In the kinetics expression, the grain radius has been calculated with the BET surface and the apparent density. An overview of the determined kinetic parameters is provided in Table 5 and the lines in Fig. 9 represent the solids conversion curves that are obtained with these kinetics. The figure shows that the derived kinetic correlation gives a good description of the experimental data.

While gas–solid kinetics can be well described after experiments in TGA, fully reduced oxygen carrier has been used for studying its gas-phase catalytic activity in fixed bed operation (see for the description Section 2.3). The measured kinetic data have been compared to the reaction scheme and kinetics proposed by Numaguchi and Kikuchi [27]. The selection of this reaction

Table 4
Expressions used for the kinetic terms.

$r_{Ni} = \frac{\varepsilon_{s,p}\rho_s\omega^0_{act}}{b\cdot M_j}\frac{dX_j}{dt}$	(1)
$\frac{dX_j}{dt} = \frac{\frac{3C^n_g}{br_0C_s}}{\left(\frac{1}{k}(1-X)^{-\frac{2}{3}}+\frac{r_0}{D}(1-X)^{-\frac{1}{3}}-\frac{r_0}{D}\right)}$	(2)
$k = k_0\exp\left[-\frac{E_A}{RT}\right]$	(3)
$D = D_0\exp\left[-\frac{E_D}{RT}\right]\exp[-k_xX]$	(4)

Table 5
Derived kinetic parameters for the $NiO/CaAl_2O_4$ particles.

	H_2	CO	O_2
C_s (mol/m^3)	89,960	89,960	151,200
r_0 (m)	$3.13\cdot10^{-8}$	$3.13\cdot10^{-8}$	$5.8\cdot10^{-7}$
k_0 (m/s)	$9.00\cdot10^{-4}$	$3.5\cdot10^{-3}$	$1.2\cdot10^{-3}$
E_A (kJ/mol)	30	45	7
n	0.6	0.65	0.9
D_0 (m^2/s)	$1.70\cdot10^{-3}$	$7.4\cdot10^{6}$	1
E_D (kJ/mol)	150	300	0
k_x	5	15	0
b	1	1	2

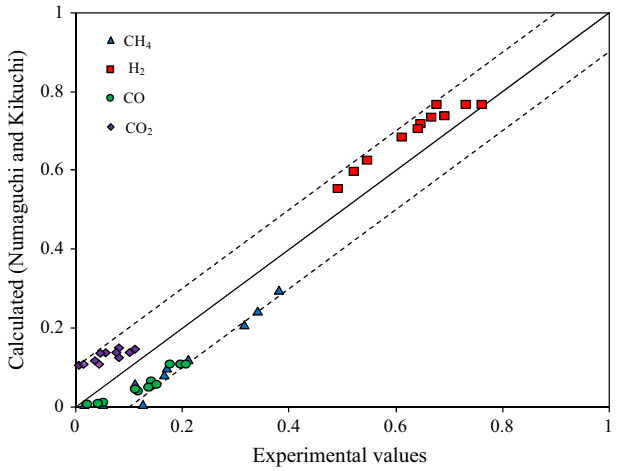

Fig. 10. Parity plot for a comparison between experimental and calculated values; points represent dry basis component molar fraction for every experiment. Dashed lines represent ± 10% of deviation respect to the perfect matching.

description is related to the fact that a similar material was used (Ni/Al_2O_3) with similar Ni content in the sample (8.7 wt%). Moreover, the temperature range used in their study is suitable for the low temperature chemical looping applications.

The catalytic reaction has been carried out under different conditions defined in Section 2.3, and results have been compared with simulated results according to the kinetic model described by Numaguchi and Kikuchi. In Fig. 10 a parity plot between our experimental results and computed results using the literature correlation for the same conditions is shown. For both cases results are presented as the dry composition of products at the outlet of the reactor. The parity plot shows that, despite some deviations for some of the cases, there is a reasonable agreement between the experimental and calculated values. It brings as a conclusion that the gas-phase catalytic behaviour of the oxygen carrier during the catalytic reforming can be well described with the kinetics proposed by Numaguchi and Kikuchi.

4. Conclusions

A Johnson Matthey Ni-based catalyst (HiFUEL® R110, available from Alfa Aesar) has been studied as oxygen carrier for novel reactor concepts based on low temperature Chemical Looping applications such as PB-CLC and MA-CLR. The oxygen carrier is supported on $CaAl_2O_4$, which avoids the formation of nickel aluminates as was confirmed by XRD analyses. Due to the absence of studies on low temperature behaviour of oxygen carriers, it has been discovered that this oxygen carrier behaves differently when it is used fresh for low temperature applications as when it is used directly for common high temperature Chemical Looping systems. Actually, this important difference can be somehow reduced via the activation of the oxygen carrier, which has been identified as an important action that should be taken prior using the oxygen carrier for the presented applications. In order to short out this issue, a procedure for the activation has been given in this work. TGA experiments have shown an increase in the oxygen carrier conversion and its kinetics after carrying out a reduction at 900 °C. It was found that after many redox cycles the nickel content was slightly reduced. Characterization of the sample has confirmed that the activation of the oxygen carrier is not related to structural changes in the morphology (BET) or the formation of new compounds (XRD). The activation of the oxygen carrier and the change in the measured Ni content on the oxygen carrier surface was investigated by TPR, XPS and SEM. The explanation for observed behaviour is related to the interaction of the Ni with the support. In fresh material a monolayer of Ni is coating the support, and this monolayer has a strong interaction with the support and partially covers a certain content of the Ni available for reaction, resulting in a decrease in the observed reaction rates compared to activated material and also lower final solid conversions. However, once the oxygen carrier is activated, a redistribution of the Ni has been observed. The monolayer turns into nickel grains that show high reactivity due to an increase in the contact area. This is also supported by the observed reduction in the binding energy for Ni^{2p} in the surface for activated material compared to fresh material. After several cycles, the activated oxygen carrier suffers somewhat from Ni agglomeration, which was observed in both XPS analyses and SEM images, where the grain size increases and hence the total amount of superficial nickel decreased. This agglomeration implies a small concomitant decrease in the oxygen carrier conversion. Despite this agglomeration, the activated oxygen carrier reactivity remains comparable to the activated material.

Thus, a $NiO/CaAl_2O_4$ catalyst was found to be a suitable oxygen carrier for low temperature Chemical Looping applications, provided that the oxygen carrier was first activated by a reduction step at 900 °C. A good description has been obtained for the gas–solid kinetics of the redox reactions with H_2, CO and O_2 at 500–800 °C and atmospheric pressure. Moreover, due to the solid also behaves as catalyst for reforming reactions, the gas-phase kinetics of the reduced material has been compared to the kinetics description proposed by Numaguchi and Kikuchi and a reasonable agreement was found. In future works, this oxygen carrier material and its kinetics descriptions will be used to investigate and evaluate novel low temperature chemical-looping applications.

Acknowledgements

Authors are grateful to NWO/STW for the financial support through the VIDI project ClingCO_2 – project number 12365.

References

[1] Archer D. Fate of fossil fuel CO_2 in geologic time. J Geophys Res 2005;110:C09S05.
[2] IPCC. IPCC special report on carbon dioxide capture and storage. Cambridge (UK): Cambridge University Press; 2005.
[3] International Energy Agency. Energy technology perspectives: scenarios and strategies to 2050. Paris (France): OECD/IEA; 2010.
[4] Toftegaard MB, Brix J, Jensen PA, Glarborg P, Jensen AD. Oxy-fuel combustion of solid fuels. Prog Energy Combust Sci 2010;36:581–625.
[5] Ishida M, Zheng D, Akehata T. Evaluation of a chemical-looping-combustion power-generation system by graphic exergy analysis. Energy 1987;12:147–54.
[6] Ishida M, Jin H. A new advanced power-generation system using chemical-looping combustion. Energy 1994;19:415–22.
[7] Lyngfelt A. Chemical-looping combustion of solid fuels–status of development. Appl Energy 2014;113:1869–73.
[8] Adanez J, Abad A, Garcia-Labiano F, Gayan P, de Diego LF. Progress in chemical-looping combustion and reforming technologies. Prog Energy Combust Sci 2012;38:215–82.
[9] Ortiz M, de Diego LF, Abad A, García-Labiano F, Gayán P, Adánez J. Hydrogen production by auto-thermal chemical-looping reforming in a pressurized fluidized bed reactor using Ni-based oxygen carriers. Int J Hydrogen Energy 2010;35:151–60.
[10] Rydén M, Lyngfelt A, Mattisson T. Chemical-looping combustion and chemical-looping reforming in a circulating fluidized-bed reactor using Ni-based oxygen carriers. Energy Fuels 2008;22:2585–97.
[11] Chiron F-X, Patience GS. Kinetics of mixed copper–iron based oxygen carriers for hydrogen production by chemical looping water splitting. Int J Hydrogen Energy 2012;37:10526–38.
[12] Cho WC, Lee DY, Seo MW, Kim SD, Kang K, Bae KK, et al. Continuous operation characteristics of chemical looping hydrogen production system. Appl Energy 2014;113:1667–74.
[13] Gopaul SG, Dutta A, Clemmer R. Chemical looping gasification for hydrogen production: a comparison of two unique processes simulated using ASPEN Plus. Int J Hydrogen Energy 2014;39:5804–17.

[14] Hamers HP, Gallucci F, Cobden PD, Kimball E, van Sint Annaland M. A novel reactor configuration for packed bed chemical-looping combustion of syngas. Int J Greenhouse Gas Control 2013;16:1–12.
[15] Medrano JA, Spallina V, van Sint Annaland M, Gallucci F. Thermodynamic analysis of a membrane-assisted chemical looping reforming reactor concept for combined H_2 production and CO_2 capture. Int J Hydrogen Energy 2014;39:4725–38.
[16] Hamers HP, Romano MC, Spallina V, Chiesa P, Gallucci F, van Sint Annaland M. Comparison on process efficiency for CLC of syngas operated in packed bed and fluidized bed reactors. Int J Greenhouse Gas Control 2014;28:65–78.
[17] Spallina V, Gallucci F, Romano MC, Chiesa P, Lozza G, van Sint Annaland M. Investigation of heat management for CLC of syngas in packed bed reactors. Chem Eng 2013;225:174–91.
[18] Kimball E, Hamers HP, Cobden P, Gallucci F, van Sint Annaland M. Operation of fixed-bed chemical looping combustion. Energy Procedia 2013;37:575–9.
[19] Angeli SD, Monteleone G, Giaconia A, Lemonidou AA. State-of-the-art catalysts for CH_4 steam reforming at low temperature. Int J Hydrogen Energy 2014;39:1979–97.
[20] Gayán P, de Diego LF, García-Labiano F, Adánez J, Abad A, Dueso C. Effect of support on reactivity and selectivity of Ni-based oxygen carriers for chemical-looping combustion. Fuel 2008;87:2641–50.
[21] Gayán P, Cabello A, García-Labiano F, Abad A, de Diego LF, Adánez J. Performance of a low Ni content oxygen carrier for fuel gas combustion in a continuous CLC unit using a CaO/Al_2O_3 system as support. Int J Greenhouse Gas Control 2013;14:209–19.
[22] Shirley D. High-resolution X-ray photoemission spectrum of valence bands of gold. Phys Rev B 1972;5:4709.
[23] Cabello A, Gayán P, García-Labiano F, de Diego LF, Abad A, Izquierdo MT, et al. Relevance of the catalytic activity on the performance of a $NiO/CaAl_2O_4$ oxygen carrier in a CLC process. Appl Catal B Environ 2014;147:980–7.
[24] Mile B, Stirling D, Zammit MA, Lovell A, Webb M. The location of nickel oxide and nickel in silica-supported catalyst: two forms of "NiO" and the assignment of temperature-programmed reduction profiles. J Catal 1988;114:217–29.
[25] Abad A, Adánez J, García-Labiano F, de Diego LF, Gayán P, Celaya J. Mapping of the range of operational conditions for Cu-, Fe-, and Ni-based oxygen carriers in chemical-looping combustion. Chem Eng Sci 2007;62:533–49.
[26] Dueso C, Ortiz M, Abad A, García-Labiano F, de Diego LF, Gayán P, et al. Reduction and oxidation kinetics of nickel-based oxygen-carriers for chemical-looping combustion and chemical-looping reforming. Chem Eng J 2012;188:142–54.
[27] Numaguchi T, Kikuchi T. Intrinsic kinetics and design simulation in a complex reaction network: steam-methane reforming. Chem Eng Sci 1988;43:2295–301.